Available online at www.eccomasproceedia.org
Eccomas Proceedia COMPDYN (2025) 7 4- 745

ECCOMAS
Proceedia

COMPDYN 2025
10th ECCOMAS Thematic Conference on
Computational Methods in Structural Dynamics and Earthquake Engineering
M. Papadrakakis, M. Fragiadakis (eds.)
Rhodes Island, Greece, 15-18 June 2025

SIMPLIFIED STRATEGIES OF FLUID VISCOUS DAMPERS' (FVDs) DESIGN FOR IN-PLANE AND IN ELEVATION IRREGULAR HYSTERETIC HIGH-RISE STRUCTURES

Maria Concetta Oddo[1], **Liborio Cavaleri**[1], **Anthea Amato**[1, 2]

[1] University of Palermo
Viale delle Scienze, Palermo, Italy
{mariaconcetta.oddo01, liborio.cavaleri, anthea.amato}@unipa.it

[2] University of Catania
Piazza Università, Catania, Italy
anthea.amato@phd.unict.it

Abstract

Among the strategies for the optimal design of Fluid Viscous Dampers, there is a procedure based on a simplified approach consisting in considering, as one of the hypotheses, the dynamic response of a structure governed by the first modal shape. The above-mentioned approach is addressed to elastic structure but, more important, also to hysteretic existing buildings and takes, during the design stage, the hysteretic dissipative capacity into account. Moreover, this approach has been validated for low-rise and mid-rise in-plane behaviour structures and results show that effectiveness is proved with a high probability of success. The present work investigates the possibility of applying this strategy to high-rise buildings irregular in-plane and in elevation and, in general, aims to prove its level of effectiveness. In detail, the approach here discussed is based on specific assumptions, for which low-rise and mid-rise in-plane behaviour structures are consistent with. But, in order to provide the reliability of the strategy on structures that do not satisfy these initial hypotheses, the simplified procedure is applied to benchmark models, subjected to appropriate families of base accelerograms, representatives of high-rise buildings irregular in-plane and in elevation, whose dynamic response is not always governed by the first modal shape. A comparison between the obtainable results and the design targets is carried out through time history analyses performed on FVDs-equipped (and non) structural nonlinear models, by a statistical analysis.

Keywords: Fluid Viscous Dampers, design strategy, hysteretic structures, seismic protection, high-rise irregular buildings.

ISSN:2623-3347 © 2025 The Authors. Published by Eccomas Proceedia.
Peer-review under responsibility of the organizing committee of COMPDYN 2025.
doi: 10.7712/120125.12686.25627

1 INTRODUCTION

Fluid viscous dampers (FVDs) have been commonly used, in the last decades, on both new structures and existing buildings, with the primary aim of limiting the dynamic response of civil structures and infrastructures, while also protecting them from excessive internal forces or excessive ductility demand [4–17]. These devices, unlike other systems used for civil structures and infrastructures, are characterized by a velocity dependent behavior, producing dissipative forces out of phase with displacements and containing the impact on the structural inherent stiffness [18]. Despite this, current codes (e.g. FEMA 356 [1]) still propose simplified approaches for the design and distribution of FVDs, assuming that seismic energy can be dissipated only by viscous damping, maintaining the structure in an elastic stage or, at most, considering the dissipation of energy due to structural damage as an equivalent damping inherent force [e.g. 2 and 3]. In doing this, any complication due to the non linearity of structures is overcome to give effective solutions for practical applications and to have rapid responses to real problems, with a sufficient degree of approximation.

The design procedure discussed here is based on a simplified approach, but the novelty lies in limiting the structural response by considering the contribution of external viscous damping (achievable through FVDs), inherent viscous damping and hysteretic damping that the structure can exhibit, sizing the external viscous dampers taking into account the rate of energy that the structure can dissipate by hysteresis, differently from the most diffused approaches based on maintaining the structural elastic behavior. Additionally, this method retains the benefits of linear analysis techniques. This approach has already been validated for low-rise and mid-rise in-plane behaviour structures, showing that effectiveness is proved with a high probability of success, as expected given the specific assumptions it is based on, for which these types of structures are consistent with. The present work investigates the possibility of applying this strategy to high-rise buildings irregular in-plane and in elevation, aiming to verify the reliability and effectiveness of the strategy for structures that do not match the initial assumptions.

The simplified procedure is applied to benchmark models, subjected to appropriate families of base accelerograms, representatives of high-rise buildings irregular in-plane and in elevation, whose dynamic response is not always governed by the first modal shape, which is one of the hypotheses. The concept of structural hysteretic dissipation is strong from the beginning of the proposed procedure: the additional damping ratio is fixed by comparing the actual ductility capacity of the structure (predicted by a pushover analysis) with the ductility demand obtained using the response spectra (of accelerations and displacements) according to the N2 method [19].

A comparison between the obtainable results and the design targets is conducted through time history analyses performed on FVDs-equipped (and non) structural nonlinear models, by a statistical analysis.

2 FLUID VISCOUS DAMPERS' CONSTITUTIVE LAW

In Eq. (1) the damper force f_i exhibited by the damper located in the i-th interstorey is expressed as:

$$f_i = C_i \cdot \left| l_i \left(\dot{u}_i - \dot{u}_{i-1} \right) \right|^{\alpha} \cdot \operatorname{sgn}\left(\dot{u}_i - \dot{u}_{i-1} \right) = C_i l_i^{\alpha} \left| \left(\dot{u}_i - \dot{u}_{i-1} \right) \right|^{\alpha} \cdot \operatorname{sgn}\left(\dot{u}_i - \dot{u}_{i-1} \right) \quad (1)$$

The force is related to the $\operatorname{sgn}\left(\dot{u}_i - \dot{u}_{i-1} \right)$, "signum" function of the interstorey velocity, through C_i and α, parameters dependent on constructive damper properties, and l_i, that gives information about how dampers are installed (equal to 1 in the case of K support braces).

Observe that the increase of the parameter C_i is associated with an increase in the maximum force exhibited by an FVD. Further, the progressive reduction of the exponent α makes the cycle force-displacement exhibited by an FVD close to a rectangle (α=1 is associated to an elliptical cycle, when α=0 the force displacement cycle is a rectangle).

Once fluid viscous dampers are installed on a plane shear type system, the n-degrees-of-freedom govern equation changes, becoming:

$$\mathbf{M}\ddot{\mathbf{u}} + \mathbf{C}\dot{\mathbf{u}} + \mathbf{R}\left(\dot{\mathbf{u}}, \alpha\right) + \mathbf{F}\left(\mathbf{u}, \dot{\mathbf{u}}\right) = \mathbf{M}\boldsymbol{\tau}\ddot{u}_g \tag{2}$$

Showing a new component, **R**, that is a vector in which the forces exhibited in the fluid viscous dampers and transferred to each storey are contained, vector **F** contains the restoring hysteretic forces, **C** is the inherent damping matrix and **τ** is the influence vector.

When α is equal to 1, ***R*** can be simply expressed as:

$$\mathbf{R}\left(\dot{\mathbf{u}}, \alpha = 1\right) = \tilde{\mathbf{C}}\mathbf{T}\dot{\mathbf{u}} \tag{3}$$

In Eq. (3), **T** is a nxn transformation diagonal matrix containing the transformation factor, while $\tilde{\mathbf{C}}$ is the matrix containing the constants (C_i) appearing in Eq (1).

3 THE PROPOSED STRATEGY

According to the N2 method, from a monotonic bilinear equivalent form of the F-δ curve, it is possible to obtain the available ductility of the system μ_a, to be compared with the demand in terms of ductility μ_d, expressed as follow:

$$\mu_a = \frac{\delta_{ua}}{\delta_e}, \quad \mu_d = \frac{\delta_{ud}}{\delta_e} \tag{4}$$

Since the denominator is the same, the comparison is between the ultimate displacement (δ_{ua}) and the corresponding demand (δ_{ud}). The strength reduction factor R_μ is:

$$R_\mu = \frac{mS_e(T^*)}{F_r} \tag{5}$$

In which F_r is the strength of the equivalent bilinear SDOF system, compared to the strength required for an elastic linear system (derived from the pseudo-acceleration response spectrum).

Depending on the natural period domain, T*, the displacement demand for an elastic linear system and for an elastic perfect plastic system characterized by a strength reduction factor R_μ are related as follows:

$$\begin{gathered} R_\mu = \left(\frac{\delta_{ud}}{\delta_e} - 1\right)\frac{T^*}{T_C} + 1; \quad 0 \le T^* < T_C \\ R_\mu = \frac{\delta_{ud}}{\delta_e}; \quad T^* \ge T_C \end{gathered} \tag{6}$$

Rewriting the latter equations, marking the dependence of $S_e(T^*)$ on the damping ratio ς, the only unknown is the damping ratio ς_{eff} corresponding to a ductility demand fixed equal to the ductility capacity:

$$\frac{mS_e(T^*,\varsigma_{eff})}{F_r}=\left(\frac{\delta_{ua}}{\delta_e}-1\right)\frac{T^*}{T_C}+1; \quad 0\le T^*<T_C$$
$$\frac{mS_e(T^*,\varsigma_{eff})}{F_r}=\frac{\delta_{ua}}{\delta_e}; \quad T^*\ge T_C \tag{7}$$

Solving Eqs. (7) means finding the best additional damping ratio expressed as a difference between the effective one and the inherent ratio of the structure in the state before the enhancement:

$$\varsigma_d=\varsigma_{eff}-\varsigma \tag{8}$$

Once obtained the best additional damping ratio it has to be related to an appropriate number and distribution of FVDs. To do this some hypotheses are taken into account: the structure has a plane shear type behaviour, dampers have a linear behaviour (namely characterized by α=1), even if α is generally not higher than 0.5, a uniform distribution of FVDs in elevation, dissipation capacity constant at each storey and defined by a scalar parameter C, the coincidence of the FVDs' velocity and the interstorey velocity. Under these hypotheses, Eq (2) can be rewritten as:

$$\mathbf{M\ddot{u}}(t)+\mathbf{C}^{(S)}\mathbf{\dot{u}}(t)+\mathbf{C}^{(D)}\mathbf{\dot{u}}(t)+\mathbf{Ku}(t)=-\mathbf{M\tau}\ddot{x}_g(t) \tag{9}$$

Where $\mathbf{C}^{(S)}$ is the structural inherent damping matrix and $\mathbf{C}^{(D)}$ is the damping matrix associated to the FVDs, that is:

$$\mathbf{C}^{(D)}=C\cdot\mathbf{P} \tag{10}$$

where P is the tridiagonal matrix, whose terms assume the following values P_{ii}:

$$P_{ii}=2\ \forall i\ne n;\ P_{nn}=1;\ P_{ij}=-1\ \forall j=i\pm1 \tag{11}$$

In which n is the number of storeys.

The last simplification is that the structural response is assumed to be governed by the first eigenvector, $\boldsymbol{\phi}_1$, so that is possible to write:

$$C=2\xi_d\omega_1\frac{\boldsymbol{\phi}_1^T\mathbf{M}\boldsymbol{\phi}_1}{\boldsymbol{\phi}_1^T\mathbf{P}\boldsymbol{\phi}_1} \tag{12}$$

Representative of the dissipation provided by all the FVDs at one storey in one direction. Even if equivalent to the simplified formula proposed by FEMA 356 [1], ξ_d in Eq. (12) has a totally different meaning since it is the exact supplemental damping ratio needed for a structure, subjected to a seismic action characterized by a specific response spectrum, that is able to show a non linear behaviour.

Once found the latter coefficient, consistent with the initial assumption of constant dissipation along the storeys, a different distribution can be useful, especially in the case of tall structures where the relative velocity at each storey can be very different. It consists in the assessment of the dissipation parameter C^* for all the n storeys, that is:

$$C^* = nC \tag{13}$$

redistributed in agreement to a different criterium, proportional to the storey shear, obtained by using the distribution coefficient

$$S_j = \frac{\frac{m_j}{h_j}}{\sum_{i=1}^{n} \frac{m_i}{h_i}} \tag{14}$$

Finally, to pass from the linear coefficient to the non linear one, the formula proposed in Code FEMA 273 and 274 is used, that is:

$$C_{nl} = \frac{C_l \cdot \left(|\dot{x}|_{\max}\right)^{1-\alpha}}{\lambda}; \; \lambda = \frac{\left[2^{2+\alpha} \cdot \Gamma^2\left(1+\frac{\alpha}{2}\right)\right]}{\pi \cdot \Gamma\left(2+\alpha\right)} \tag{15}$$

where $|\dot{x}|_{\max}$ is the maximum absolute value of the damper velocity.

4 DESIGN STRATEGY VALIDATION

The proposed approach has been validated for low-rise and mid-rise structures with in-plane behavior, as well as in-plane non-regular buildings, from a probabilistic perspective. This validation involved observing the dynamic responses of benchmark structures under families of accelerograms that match specific target spectra, in scenarios with nominal capacity-demand ratios derived using the N2 method. For these buildings’ classes, it provides a solution, in terms of distribution and capacity of linear fluid viscous dampers, able to guarantee, at least, a 95% of probability to obtain a capacity-demand ratio higher than 1, in some cases it reaches 100% by changing linear devices in non linear ones. Also, the similar results obtained for the class of in-plane nonregular buildings prove that the simplified assumptions used in designing the FVDs do not detract from an optimal solution and do not reduce the probability of success.

In this study, the reliability of the proposed FVDs' design strategy is evaluated for high-rise structures with hysteretic irregular behavior both in-plane and in elevation. Two different benchmark structures are analyzed: the first is a high-rise building with regular in-plane behavior and elevation, while the second exhibits irregularities in both plane and elevation, deviating from the initial assumptions. The choice to prove the effectiveness of the procedure on various types of structures derives from the awareness that the characteristics observed in practical applications may differ from those used to define the discussed approach.

Therefore, examining results from different classes of structures, which may not necessarily adhere to the initial assumptions, is essential to understanding the applicability of the proposed procedure.

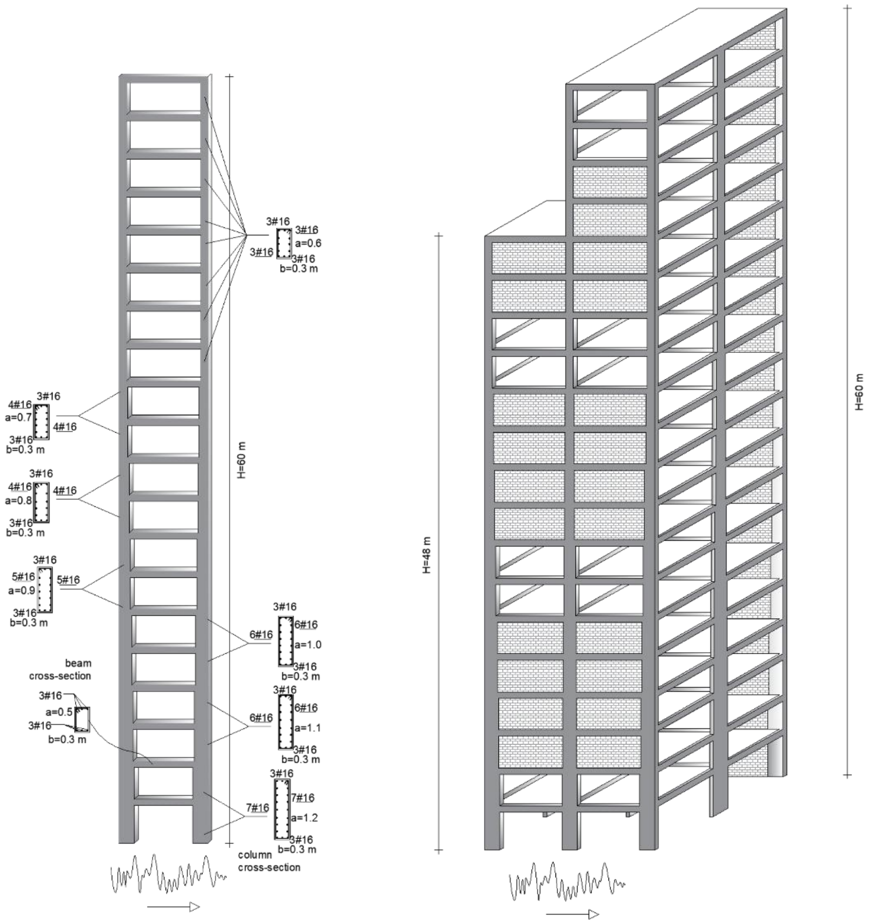

Fig. 1 - Benchmark models: a) plane high-rise regular structure; b) high-rise irregular structure

The first structure represents high-rise buildings that are regular in both plan and elevation, and it was studied to verify the strategy's reliability on structures not always governed by the first modal shape. But, the proposed strategy assumes a plane behaviour as hypothesis so the second structure, which is particularly useful for this study, is characterized by irregularity, deviating from the initial assumptions. It is derived from the first structure, maintaining the same column sections but with opposite orientation along the middle frame, and it is equipped with non-symmetrical infills that create significant in-plane irregularity (equivalent pin-jointed diagonal struts, using a linear, indefinite elastic material in Fig. 2).

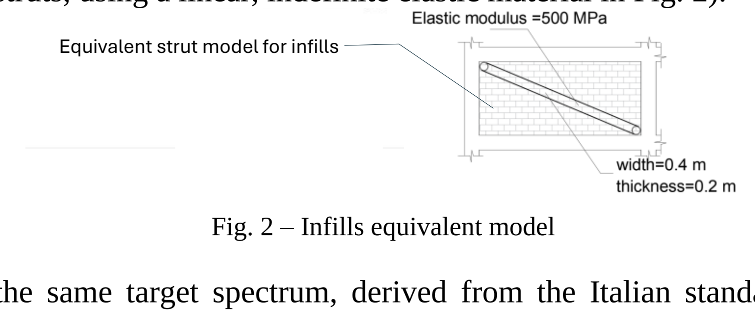

Fig. 2 – Infills equivalent model

Considering the same target spectrum, derived from the Italian standards, for both the structural models, two levels of the nominal capacity-demand ratio (C/D) in terms of top displacements have been found, 0.67 for the regular structure and 0.53 for the irregular one. A preliminary pushover analysis for both the benchmark structures has been performed, obtaining the bilinear base shear-top displacement curves, as shown in Fig. 3.

The non linear behaviour is expressed through cross section shown in Fig. 1, assumed as fiber section and the materials showing the following constitutive law:

- for concrete Mander (backbone) model and Takeda hysteresis model for cyclic behaviour (f_{cc} 20 MPa, f_2 10.4 MPa; ε_{cc} 0.0013, ε_{cu} 0.005);
- for steel Kinematic hysteresis model for cyclic behaviour (f_{sy} 450 MPa, f_{su} 530 MPa; ε_{sy} 0.0021, ε_{su} 0.675)

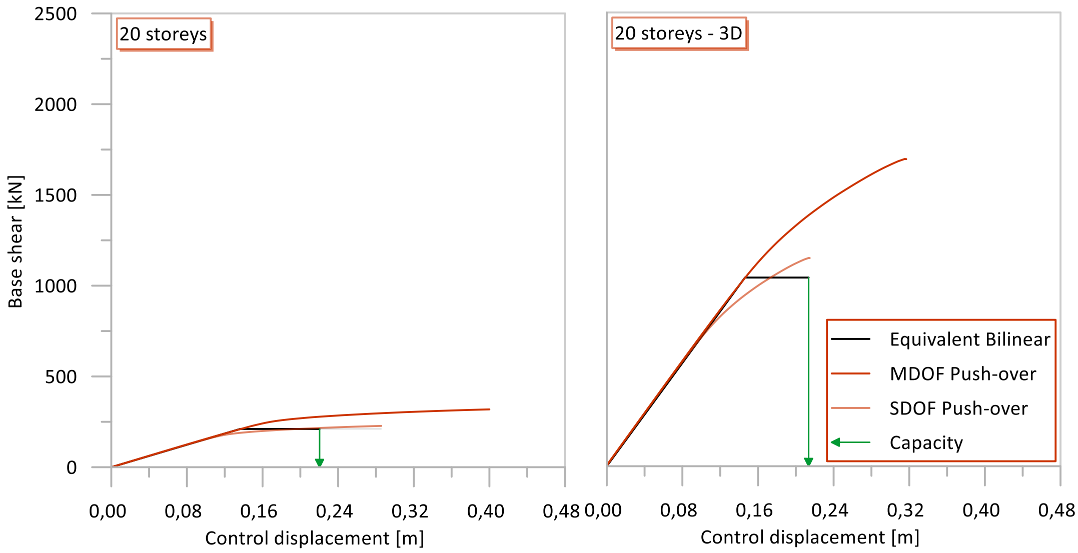

Fig. 3 - Benchmark models' MDOF, SDOF and Bilinear structural responses

In Fig. 4 are shown the ADRS used to obtain the capacity-demand ratios and the equivalent force-displacement bilinear curves for each benchmark structure.

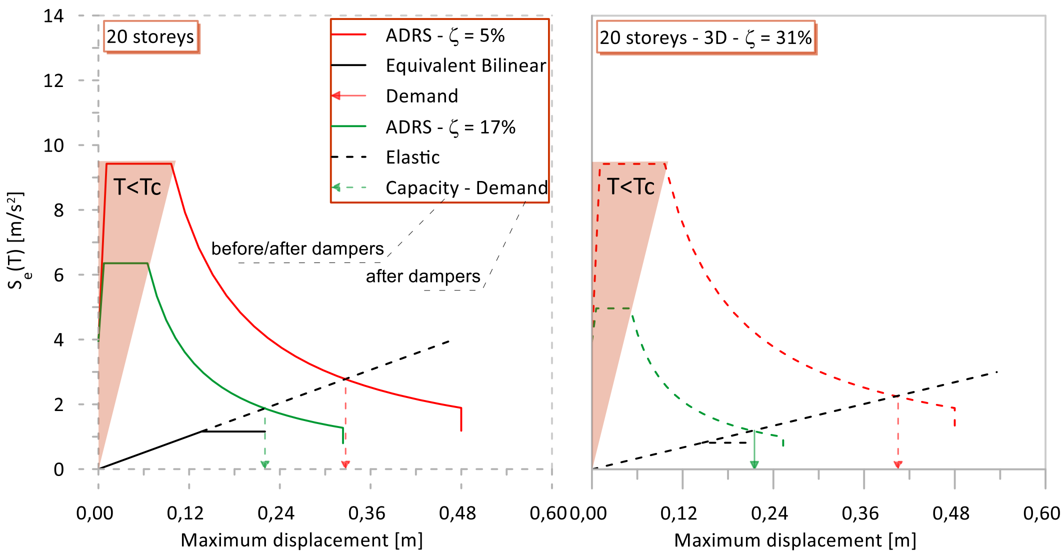

Fig. 4 - ADRS with and without (ζ=5%) fluid viscous dampers (PGA=0.4g), mass normalized bilinear structural responses

Bilinear structural responses and the response spectra are mass normalized for an easier comparison. It is possible to notice that each model is characterized by a fundamental period T higher than T_c, so that the response elastic branch encounters the response spectrum in its third branch.

To probabilistically assess the procedure by observing and processing the results of dynamic analyses before and after the introduction of fluid viscous dampers 50 accelerograms have been generated and applied to the benchmark models. The target spectrum and the spectra from the accelerograms (chosen in such a way that the corresponding response spectrum provided, on average, the PGA associated with the target spectrum) used for the dynamic analyses have been extrapolated and are here proposed.

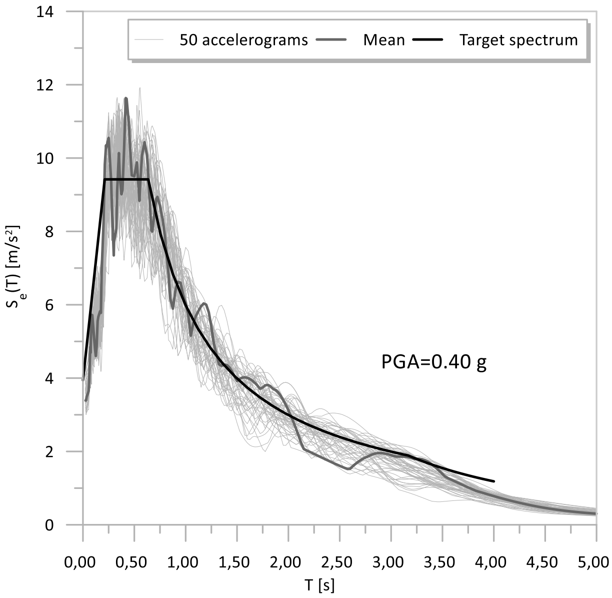

Fig. 5 - Target spectrum and spectra from the accelerograms comparison

Table 1 shows all the parameters used in the analyses, in particular values of the additional damping ζ_d obtained by Eqs. (7) and (8) (graphically obtained in Fig. 4), the dissipation parameters constant along the storeys, the first and the last storey values when the latter is assigned according to the storey shear distribution, and for these three values the corresponding non linear parameters when α=0.15. Last but not least since it is representative of one of the initial assumptions, the participation mass associated to the modal shape used for the estimation of the damper parameters has been also inserted.

Table 1 - Additional damping ζ_d and corresponding FVDs' parameters values, modal shape participation mass

ζ_d [%]	$C_{lc}\left[kN\cdot\frac{s}{m}\right]$	$C_{nlc}\left[kN\cdot\left(\frac{s}{m}\right)^{0.15}\right]$	$C_{lp}\left[kN\cdot\frac{s}{m}\right]$ Bottom Storey	Top storey	$C_{nlp}\left[kN\cdot\left(\frac{s}{m}\right)^{0.15}\right]$ Bottom Storey	Top storey	Participating Mass
20 *Storeys*							
12	1378	78	8007	345	415	19	70%
20 *Storeys* − 3*D*							
26	11923	570	68755	3045	3286	145	73%

The capacity demand ratio has been chosen as random variable, so from each analyses the capacity and the demand with and without additional damping, variously simulated, have been extracted and the probabilistic distribution, assumed as lognormal, has been generated.

In Table 2, mean and standard deviation of the capacity-demand ratios are inserted for comparison.

Table 2 - Capacity-demand ratios' mean and standard deviation obtained from 50 dynamic analyses.

	Capacity/Demand	
	Mean	Standard Deviation
20 Storeys		
ID - Inherent Damping (5%)	0,758	0,273
ID - Inherent Damping (17%)	1,178	0,152
ALD - Uniform Distribution	0,910	0,177
ANLD – Uniform Distribution	0,922	0,164
ALD – Storey Shear Distribution	0,947	0,115
ANLD – Storey Shear Distribution	0,939	0,118
20 Storeys – 3D		
ID - Inherent Damping (5%)	0,406	0,199
ID - Inherent Damping (26%)	1,065	0,154
ALD - Uniform Distribution	0,691	0,219
ANLD – Uniform Distribution	0,716	0,221
ALD – Storey Shear Distribution	0,959	0,105
ANLD – Storey Shear Distribution	0,925	0,110

In Fig. 6, the capacity-demand distributions are inserted.

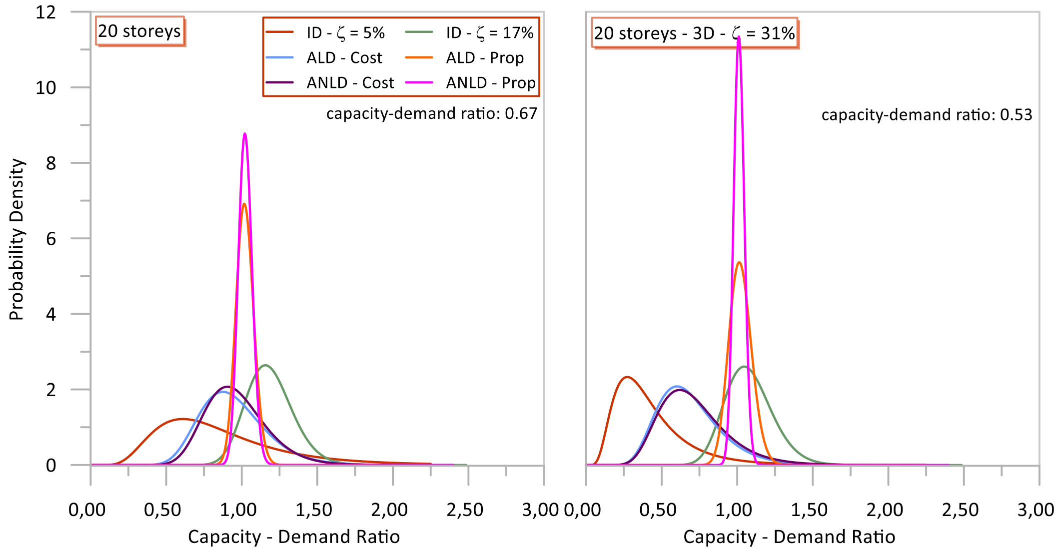

Fig. 6 - Capacity-demand ratio probability density distributions with and without additional damping (ID-ζ=5%: original structure with inherent damping 5%; ID-ζ=17% / 31%: structure with inherent damping 17% / 31%:; ALD-Cost: linear dampers uniformly distributed along the storeys; ANLD-Cost: nonlinear dampers uniformly distributed along the storeys; ALD-Prop: linear dampers distributed according to the storey shear; ANLD-Prop: nonlinear dampers distributed according to the storey shear).

What emerges is that both systems show approximately the same response: the most frequent value of capacity-demand ratio obtained by the analyses conducted on the structure without additional damping is lower than the one obtainable by the pushover analysis, especially for the irregular structure, it was expected since pushover analysis provides a range for the capacity-demand ratio. Also, nonlinear dampers are much more effective than linear dampers, especially if distributed according to the storey shear.

In both cases, linear and nonlinear additional damping uniform along the storeys does not cause a sufficient increase in the capacity, leaving approximately a probability of 50% of collapse. This circumstance is much clearer by the observation of the cumulative density functions in Fig. 7.

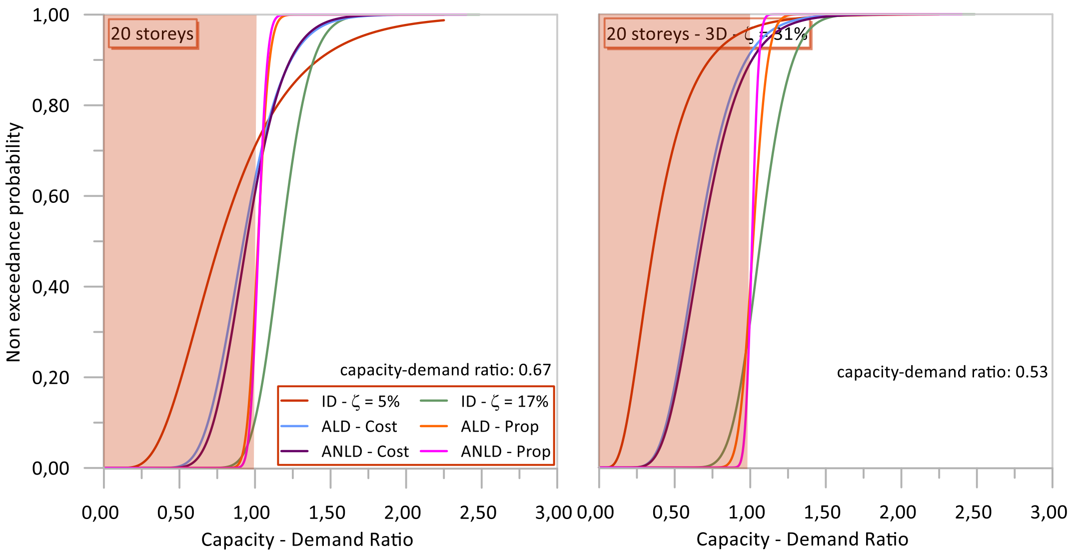

Fig. 7 - Capacity-demand ratio cumulative probability distributions with and without additional damping (legend in caption of Fig. 6)

In fact, only a non-uniform distribution of nonlinear dampers can consistently ensure a probability of occurrence lower than 5% for a capacity-to-demand ratio less than 1. This is evident from the overlapping cumulative probability functions and the area in the non-exceedance probability-capacity-demand ratio plot. It is important to note the difference in the probability distribution of capacity-demand ratios when additional damping is considered as inherent damping within the structure versus when it is considered as concentrated damping proved by fluid viscous dampers. This distinction is highlighted to emphasize that, during the design stage, additional damping is assumed to be inherent distributed damping, unlike the post-design stage where concentrated damping is introduced at each storey.

5 CONCLUSIONS

Previous sections proved that it is possible to name FVDs among the most effective seismic protection systems for existing buildings, not only for low-rice and mid-rice structures, but also for high-rise regular and irregular systems. The novelty is that in the design phase the additional amount of energy dissipation capability adds to the natural capability of structural systems to dissipate through inherent viscosity and hysteresis mechanisms, starting from a comparison between capacity and demand of a system subjected to a particular earthquake, using the N2 method. Considering the correlation between indefinitely linear systems and elastic-plastic systems, the exact amount of additional dissipation can be found.

The procedure reliability has been valued for high-rice building through a probabilistic assessment and the results obtained have come into some important considerations:

- Linear and nonlinear additional damping uniform along the storeys does not cause a sufficient increase in the capacity, leaving approximately a probability of 50% of collapse, this could be related to the systems' dynamic responses not governed by the first modal shape;

- Non linear dampers are more effective than linear ones, especially if distributed along the storeys;
- Non uniform distribution is the most appropriate for high-rice structures, regular and irregular;
- The initial assumptions do not affect the probability of success since a capacity demand ratio higher than 1 can be reached in the case of non uniform distribution.

ACKNOWLEDGMENTS

This study was carried out within the RETURN Extended Partnership and received funding from the European Union Next-GenerationEU (National Recovery and Resilience Plan – NRRP, Mission 4, Component 2, Investment 1.3 – D.D. 1243 2/8/2022, PE0000005)

REFERENCES

[1] Federal Emergency Management Agency (FEMA) and American Society of Civil Engineers (ASCE). Prestandard and commentary for the seismic rehabilitation of buildings. Report FEMA-356, Washington, DC, November 2000.

[2] N. Impollonia, A. Palmeri, Seismic performance of buildings retrofitted with nonlinear viscous dampers and adjacent reaction towers. *Earth Eng Struct Dyn*, **47(5)**, 1329–1351, 2018.

[3] S. Wang, S.A. Mahin, High-performance computer-aided optimization of viscous dampers for improving the seismic performance of a tall building. *Soil Dyn Earth Eng*, **113**, 454–461, 2018.

[4] X. Liu, W. Wang, J. Li, Full-Scale Shaking Table Tests and Numerical Studies of Structural Frames with a Hybrid Isolation System. *Eng Struct*, **292**, 116545, 2023.

[5] R. Ullah, M. Vafaei, S.C. Alih, A. Waheed, A Replaceable Sandwiched Metallic Fuse Damper for Seismic Protection of Braced Frames. *Eng Struct*, **298**, 117072, 2024.

[6] G. Terenzi, Energy-Based Design Criterion of Dissipative Bracing Systems for the Seismic Retrofit of Frame Structures. *Appl Sci*, **8**, 268, 2018.

[7] E. Parcianello, C. Chisari, C. Amadio, Optimal Design of Nonlinear Viscous Dampers for Frame Structures. *Soil Dyn Earth Eng*, **100**, 257–260, 2017.

[8] Y.X. Hui, L.S. Li, H. Cheng, Y.J. Zhang, D.S. Wang, Seismic Mitigation of Continuous Girder Bridges Equipped with U-Shaped Stainless Steel Dampers under near-Fault Earthquake Excitations, *Struct*, **58**, 105597, 2023.

[9] X. Xu, X. Chen, H. Hu, X. Zhou, M. Cheng, L. Sun, X. Li, Energy Dissipation and Seismic Response Reduction System for High-Speed Railway Bridges Based on Multiple Performance Requirements. *Eng Struct*, **307**, 117919, 2024.

[10] J. Fu, S. Wan, P. Zhou, J. Shen, M. Loccufier, K. Dekemele, Effect of Magnetic-Spring Bi-Stable Nonlinear Energy Sink on Vibration and Damage Reduction of Concrete Double-Column Piers: Experimental and Numerical Analysis. *Eng Struct*, **303**, 117517, 2024.

[11] J. Li, L. Xu, Seismic Performance Improvement of Continuous Rigid-Frame Bridges with Hybrid Control System under near-Fault Ground Motions. *Soil Dyn Earth Eng*, **168**, 107858, 2023.

[12] K.V. Sharma, V. Parmar, L. Gautam, S. Choudhary, J. Gohil, Modelling Efficiency of Fluid Viscous Dampers Positioning for Increasing Tall Buildings' Resilience to Earthquakes Induced Structural Vibrations. *Soil Dyn Earth Eng*, **173**, 108108, 2023.

[13] T. Guo, J. Xu, W. Xu, Z. Di, Seismic Upgrade of Existing Buildings with Fluid Viscous Dampers: Design Methodologies and Case Study. *J Perform Constr Facil*, **29**, 04014175, 2015.

[14] M.D. Symans, F.A. Charney, A.S. Whittaker, M.C. Constantinou, C.A. Kircher, M.W. Johnson, R.J. McNamara, Energy Dissipation Systems for Seismic Applications: Current Practice and Recent Developments. *J Struct Eng*, **134**, 3–21, 2008.

[15] M.F. Ferrotto, L. Cavaleri, Variable Friction Dampers (VFD) for a modulated mitigation of the seismic response of framed structures: Characteristics and design criteria. *Prob Eng Mechs*, **70**, 103375, 2022.

[16] M.F. Ferrotto, M. Di Paola, L. Cavaleri, Seismic behavior of structures equipped with variable friction dissipative (VFD) systems. *Bull Earthq Eng*, **19(11)**, 4623–4639, 2021.

[17] L. Cavaleri L, F. Di Trapani, M.F. Ferrotto, Experimental determination of viscous damper parameters in low velocity ranges. *Int J Earthq Eng*, **34(2)**, 64 – 74, 2017.

[18] D. De Domenico, G. Ricciardi, I. Takewaki, Design Strategies of Viscous Dampers for Seismic Protection of Building Structures: A Review. *Soil Dyn Earth Eng*, **118**, 144–165, 2019.

[19] S. Fajfar, *The Story of the N2 method*. IAEE, 2021.